

J/ψ and Υ Polarization in Hadronic Production Processes

Eric Braaten

Department of Physics, The Ohio State University, Columbus, OH 43210, USA

James Russ

*Physics Department,
Carnegie-Mellon University,
Pittsburgh, PA 15213, USA*

Abstract

Both charm and bottom quarks form nonrelativistic bound states analogous to positronium. The J/ψ and $\psi(2S)$ charmonium states and the first three $\Upsilon(nS)$ bottomonium states, all spin-triplet S -wave quarkonium states below open-heavy-flavor thresholds, have relatively large branching ratios to e^-e^+ or $\mu^-\mu^+$ pairs. In hadron collisions, experiments measuring lepton pairs can determine polarization by using angular correlation techniques. The polarization, in turn, can be related theoretically to the production mechanism for the bound state. This review summarizes experimental studies with proton beams at fixed target and colliding beam accelerators, covering a center-of-mass energy range from 39 to 7000 GeV for nucleon and antiproton targets. Analyses using various polarization frames and spin-quantization axes are described and results compared. A pattern emerges that connects experimental results over the whole energy span. The theoretical implications of the pattern are presented and a set of new measurements is proposed.

Prepared for Volume 64 of the Annual Review of Nuclear and Particle Science

I. INTRODUCTION

Photon *polarization* has long been used to determine the properties of electromagnetic transition matrix elements. Measuring the polarization properties of the Cosmic Background Radiation is expected to provide strong constraints on models of the early universe [1]. Polarization measurements may play a crucial role in determining the spin of any new heavy particles discovered at the Large Hadron Collider. The power of polarization measurements is that they can follow changes in the matrix elements that contribute to a complex process as kinematic variables change.

This review treats recent developments in polarization measurements for *quarkonium* systems produced in hadronic collisions. These mesons are bound states of heavy-flavor quarks, $c\bar{c}$ or $b\bar{b}$. They exhibit a positronium-like series of excited states with increasing principal and orbital-angular-momentum quantum numbers, shown for bottomonium in Fig. 1. The spin-triplet S -wave states of quarkonium, which have J^{PC} quantum numbers 1^{--} , can decay into a pair of leptons through a virtual photon. The dilepton angular distribution can be used as a probe of the quarkonium polarization in hadronic production processes.

The goal of quarkonium polarization measurements in high-energy hadron collisions is to determine the mechanisms by which a heavy quark-antiquark pair is produced by parton-parton collisions and by which it subsequently binds into a colorless meson H . The relevant kinematic variables for inclusive production of H are its *transverse momentum* p_T and a longitudinal variable,¹ either its *rapidity* y or its *Feynman variable* x_F . Despite the complexity of describing strong production processes using *Quantum Chromodynamics* (QCD), two simplifications arise for quarkonium production due to the heavy quark's mass being much larger than the light-quark interaction energy scale Λ_{QCD} . First, the *asymptotic freedom* of the QCD coupling constant allows the creation of the heavy quarks to be described perturbatively, provided also that the quarkonium state H has sufficient transverse momentum to suppress interactions of the heavy quarks with the light-parton remnants of the colliding hadrons. Second, the nonrelativistic velocities of the heavy quarks in the rest frame of H simplify the nonperturbative dynamics of the formation of the bound state. The spin structure of the matrix element for the parity-conserving electromagnetic decay into leptons is completely determined by Lorentz invariance. The decay angular distribution of the leptons carries information about the spin density matrix for the vector quarkonium and therefore about the process by which that quarkonium was produced. Experiments can determine the variation of the decay angular distribution with kinematic variables. Theory has to provide the interpretive framework to relate the data to the dominant matrix elements for the production process. This review will consider the present state of both sides of this interpretive equation.

We recall that precision experiments are difficult. The record of experimental science shows that the first measurements of any important observable are sometimes not consistent with later, more sophisticated measurements made with larger data samples. We will review the available polarization experiments and their phase space coverage with an eye toward identifying the strengths of each. At the end, we will summarize the situation and identify what we know experimentally about quarkonium polarization. We give potential theoretical

¹ Rapidity y and Feynman x_F are different longitudinal kinematic variables for a hadron: $y \equiv \frac{1}{2} \ln[(E + \vec{p} \cdot \hat{z}) / (E - \vec{p} \cdot \hat{z})]$, where E and \vec{p} are its energy and momentum in the center-of-momentum frame of the colliding hadrons and \hat{z} is the collision axis, while $x_F = \vec{p} \cdot \hat{z} / p_{\text{max}}$. At $y = 0$, $x_F = 0$.

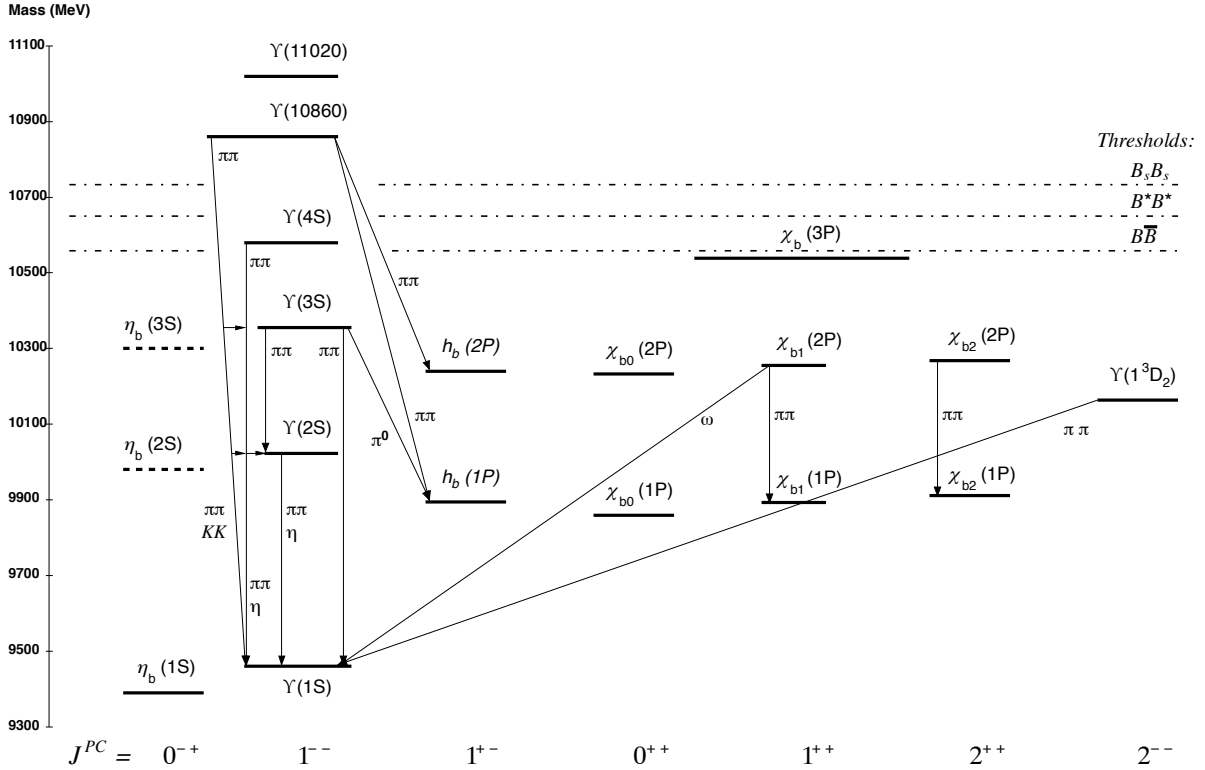


FIG. 1: Bottomonium bound states and their observed hadronic transitions.

implications of the global trends of the measurements to date. Finally, we will review important next steps to be taken to improve our knowledge of the hadroproduction of quarkonium.

II. POLARIZATION FRAMES

The polarization of a spin-triplet S -wave quarkonium state can be revealed by the angular distribution of the lepton pair into which it decays. In this section, we discuss the polarization frames that can be used to define that angular distribution.

A. Angular Distributions

In the rest frame of a vector meson, its spin component along any *spin-quantization axis* has three possible eigenvalues: $m_s = 0, \pm 1$ (in units of \hbar). The $m_s = 0$ state is called *longitudinal* and the $m_s = \pm 1$ states are called *transverse*. Because of the parity symmetry of QCD, a collision of unpolarized hadrons cannot produce a vector meson with different probabilities for the spin states $+1$ and -1 . We will consider a vector meson to have a net *polarization* if the probabilities for a single transverse spin state and the longitudinal spin

state differ.²

When a vector meson decays into a lepton pair, its polarization is reflected in the angular distribution of the leptons, as specified, e.g., in terms of the spherical angles θ and ϕ for the momentum vector of the positively charged lepton in the rest frame of the vector meson. In order to define those angles, it is necessary to choose a *polarization frame*. The angle θ is the polar angle with respect to the spin-quantization axis. An orthogonal axis in the collision plane must be specified to define the zero of the azimuthal angle. For inclusive hadroproduction of a vector meson, the only available vectors are the momenta of the vector meson and the colliding hadrons. In the rest frame of the vector meson, the two orthogonal axes lie in the collision plane defined by the boosted momenta of the colliding hadrons.

A thorough discussion of the dilepton angular distribution and quarkonium polarization has been presented by Faccioli *et al.* [2]. The most general angular distribution for the dileptons from the decay of vector mesons produced by parity-invariant interactions is specified by three polarization parameters: λ_θ , λ_ϕ , and $\lambda_{\theta\phi}$. The two-dimensional angular distribution is

$$\frac{dW}{d(\cos\theta)d\phi} = \frac{3[1 + \lambda_\theta \cos^2\theta + \lambda_\phi \sin^2\theta \cos(2\phi) + \lambda_{\theta\phi} \sin(2\theta) \cos\phi]}{4\pi(3 + \lambda_\theta)}. \quad (1)$$

The angular distribution has been normalized so that it integrates to 1. The general constraints on the three polarization parameters are $|\lambda_\theta| \leq 1$, $|\lambda_\phi| \leq (1 + \lambda_\theta)/2$, and $\lambda_{\theta\phi}^2 \leq (1 - \lambda_\theta)(1 + \lambda_\theta - 2\lambda_\phi)/4$ [3].

The three polarization variables λ_θ , λ_ϕ , and $\lambda_{\theta\phi}$ can be determined from measurements of the one-dimensional distributions obtained by projecting the two-dimensional distribution in Eq. 1 onto $\cos\theta$, ϕ , or another angle defined by $\tilde{\phi} = \phi - \frac{1}{4}\pi[2 - \text{sign}(\cos\theta)]$ [2]:

$$\frac{dW}{d(\cos\theta)} = \frac{3}{2(3 + \lambda_\theta)} [1 + \lambda_\theta \cos^2\theta], \quad (2)$$

$$\frac{dW}{d\phi} = \frac{1}{2\pi(3 + \lambda_\theta)} [3 + \lambda_\theta + 2\lambda_\phi \cos(2\phi)], \quad (3)$$

$$\frac{dW}{d\tilde{\phi}} = \frac{1}{2\pi(3 + \lambda_\theta)} [3 + \lambda_\theta + \sqrt{2} \lambda_{\theta\phi} \cos\tilde{\phi}]. \quad (4)$$

In experiments with low statistics, it may be necessary to determine λ_θ , λ_ϕ , and $\lambda_{\theta\phi}$ from measurements of the three separate one-dimensional distributions in Eqs. 2, 3, and 4 in order to obtain stable results. In experiments with higher statistics, the three polarization parameters can be determined with smaller systematic errors from measurements of the two-dimensional distribution in Eq. 1. The statistics in those measurements can be improved by exploiting two symmetries of the angular distribution in Eq. 1: $\phi \rightarrow -\phi$ and $(\theta, \phi) \rightarrow (\pi - \theta, \pi - \phi)$. They allow the two-dimensional distribution to be folded into the first quadrant, *as long as the apparatus acceptance and efficiency are also symmetric under these two operations*.

A different choice for the polarization frame can be obtained by a rotation of the collision plane in the rest frame of the vector meson. The angular distribution in the new frame has

² Some physicists reserve the term *polarization* for situations in which the spin states $+1$ and -1 have unequal probabilities. Situations in which the probabilities for $+1$ and -1 are equal but different from that for $m_s = 0$ are called *spin alignment*.

the same general form as in Eq. 1, but with different polarization parameters λ_θ , λ_ϕ , and $\lambda_{\theta\phi}$ that are functions of the old polarization parameters and the rotation angle. There are combinations of the polarization parameters that are independent of this rotation angle:

$$\tilde{\lambda} = \frac{\lambda_\theta + 3\lambda_\phi}{1 - \lambda_\phi}, \quad (5)$$

$$\tilde{\lambda}' = \frac{(\lambda_\theta - \lambda_\phi)^2 + 4\lambda_{\theta\phi}^2}{(3 + \lambda_\theta)^2}. \quad (6)$$

The invariance of $\tilde{\lambda}$ was pointed out by Faccioli *et al.* [4, 5]. The invariance of $\tilde{\lambda}'$, which depends on all three polarization parameters, was pointed out by Palestini [3]. These two frame-invariant polarization parameters provide powerful constraints on the accuracy of measurements of the dilepton angular distributions in different polarization frames. They could also be useful in theoretical calculations to check whether error estimates on predictions of the polarization are underestimated.

Because the same data are used in evaluating polarization variables in each frame, comparing the frame-independent quantities from two frames cannot be based on the statistical uncertainties, which are highly correlated. Generally, a Monte Carlo study of the range of expected variation is used to determine the consistency of comparisons of $\tilde{\lambda}$ or $\tilde{\lambda}'$ for different frames.

B. Specific Polarization Frames

The polarization frame can be specified by the direction of the spin-quantization axis in the plane containing the momentum vectors of the colliding hadrons in the quarkonium rest frame. There are several choices for the spin-quantization axis in the literature:

- **Gottfried-Jackson** (GJ) axis [6]: the direction of the momentum of one of the two colliding hadrons,
- **Collins-Soper** (CS) axis [7]: the direction of the difference between the velocity vectors of the colliding hadrons,
- **center-of-mass helicity** (cm-helicity) axis: the direction of the boost required to go from the quarkonium rest frame to the center-of-momentum frame of the colliding hadrons,
- **perpendicular helicity** (\perp -helicity) axis [8, 9]: the direction of the sum of the velocity vectors of the colliding hadrons or, alternatively, the direction of the boost required to go from the quarkonium rest frame to the frame in which the quarkonium momentum is perpendicular to the axis of the colliding hadrons.

For some of these frames, there are simple physical mechanisms that tend to produce polarization in spin-triplet S -wave quarkonium [2, 9]. If the $Q\bar{Q}$ pair is created directly by a virtual gluon or virtual photon from the collision of a massless quark and antiquark that are collinear with the colliding hadrons, the polarization will tend to be transverse in the CS frame and longitudinal in the cm-helicity frame. The transverse polarization in the CS frame follows from the helicity conservation of the interaction of the virtual gluon or photon

with the light quark and antiquark. If the $Q\bar{Q}$ pair is created directly by a virtual gluon or virtual photon with transverse momentum that is much larger than the heavy quark mass, the polarization of quarkonium will tend to be transverse in the cm-helicity and \perp -helicity frames. The transverse polarization follows from the approximate helicity conservation of the interaction of the almost on-shell gluon or photon with the heavy quark and antiquark.

The polarization parameter λ_θ measures the degree of polarization with respect to the spin-quantization axis. It can be expressed as $(\sigma_T - 2\sigma_L)/(\sigma_T + 2\sigma_L)$, where σ_T and σ_L are the cross sections for the two transverse states and for the single longitudinal state, respectively. A vector meson can be polarized with respect to one quantization axis and unpolarized with respect to another. Measurements of λ_θ with respect to two orthogonal spin-quantization axes carries much more information about the polarization mechanism than a single measurement [10]. If $\lambda_\theta = 0$ for both frames, then $\lambda_\phi = 0$ for both frames and $\lambda_{\theta\phi}$ is equal and opposite in the two frames. At zero rapidity, the CS axis is orthogonal to the cm-helicity axis, which coincides with the \perp -helicity axis. The CS and \perp -helicity axes remain orthogonal at nonzero rapidity, so measurements of λ_θ with respect to these two axes will provide the most information about the polarization mechanism [8, 9].

III. THEORETICAL CONSIDERATIONS

In this section, we describe various theoretical approaches to quarkonium production in QCD and discuss their implications for polarization.

A. General considerations

Because of the asymptotic freedom of the QCD coupling constant, amplitudes involving a large momentum transfer Q can be calculated using perturbative QCD (pQCD) as an expansion in powers of $\alpha_s(Q)$, provided there is a factorization theorem that guarantees the insensitivity of the amplitude to much smaller momentum scales. The creation of a $Q\bar{Q}$ pair in a collision of light partons involves a momentum transfer of order m_Q , where m_Q is the heavy-quark mass. The creation of a $Q\bar{Q}$ pair with transverse momentum p_T much larger than m_Q involves a momentum transfer of order p_T . In an amplitude involving large p_T , some factors of the QCD coupling constant should be $\alpha_s(p_T)$, while others may more appropriately be $\alpha_s(m_Q)$. If the momentum scales m_Q and p_T are not separated, the momentum scales in all factors of α_s are usually set to a common value, such as $(m_Q^2 + p_T^2)^{1/2}$. In a pQCD calculation, we will refer to the first few terms in the expansion in powers of α_s as leading order (LO), next-to-leading order (NLO), and next-to-next-to-leading order (N²LO).

When $p_T > m_Q$, a pQCD cross section for producing a $Q\bar{Q}$ pair with small relative momentum can, up to logarithms of p_T/m_Q , be expanded in powers of m_Q/p_T , where m_Q is the heavy-quark mass. Because QCD has asymptotic scale invariance at large momentum transfer, the leading power (LP) in $d\sigma/dp_T^2$ must, by dimensional analysis, be $1/p_T^4$. In a cross section that is summed over the quarkonium spin states, the next-to-leading power (NLP) is m_Q^2/p_T^6 . The cross sections for individual quarkonium spin states can also have the intermediate power m_Q/p_T^5 .

The formation of a quarkonium H from a $Q\bar{Q}$ pair with small relative momentum is an inherently nonperturbative process, but there are simplifications that arise from the Q and

\bar{Q} being nonrelativistic in the rest frame of H . The relative importance of nonperturbative transitions of the $Q\bar{Q}$ pair is determined by how their amplitudes scale with the relative velocity v of the Q and \bar{Q} . The typical relative velocity of the $c\bar{c}$ pair in the J/ψ is given roughly by $v^2 \approx 0.3$. The typical relative velocity of the $b\bar{b}$ pair in the $\Upsilon(1S)$ is given roughly by $v^2 \approx 0.1$. The typical relative velocities in the radially excited states are larger, but they may still be small enough to allow scaling with v to be useful as an organizing principle for nonperturbative transitions of the $Q\bar{Q}$ pair.

Nonrelativistic QCD (NRQCD) is an effective field theory for the sector of QCD that includes a nonrelativistic heavy quark and antiquark. The Lagrangian for NRQCD includes infinitely many terms, but they can be organized according to how their contributions to the energy of quarkonium scale with the typical relative velocity of the $Q\bar{Q}$ pair [11]. The leading terms of order v^2 give splittings between the radial and orbital-angular-momentum excitations of quarkonium. The terms of order v^4 give splittings within orbital-angular-momentum multiplets. By including terms of increasingly higher order in v , the spectrum of quarkonium in QCD can be reproduced with increasingly higher accuracy. NRQCD can also be used to organize nonperturbative effects in the annihilation decays of quarkonium and in the inclusive production of quarkonium [12].

An important qualitative feature of the nonrelativistic dynamics of a heavy quark is the suppression of spin flip. The amplitudes for transitions of the $Q\bar{Q}$ pair in which the spin state of the Q or \bar{Q} changes are suppressed by a factor of v^2 . Because of this suppression, the hadronic and electromagnetic transitions of an excited spin-triplet quarkonium state are primarily to lower spin-triplet states. The suppression of spin flip for a heavy quark also has implication for production of quarkonium. If the parton collisions that create a $Q\bar{Q}$ pair with small relative momentum give it a nonzero polarization, the subsequent binding of the $Q\bar{Q}$ pair will tend to preserve its spin state, passing the polarization on to the quarkonium.

B. Theoretical approaches

1. NRQCD Factorization Formula

The NRQCD factorization formula [12] is a conjectured factorization formula in which nonperturbative effects associated with the binding of a $Q\bar{Q}$ pair into quarkonium are organized into multiplicative constants. The theoretical status of the conjecture is discussed in Ref. [13]. The NRQCD factorization formula states that the inclusive cross section for producing a quarkonium state H in the collision of the light hadrons A and B can be expressed as the sum of inclusive pQCD cross sections for producing a $Q\bar{Q}$ pair multiplied by *NRQCD matrix elements*:

$$d\sigma[A + B \rightarrow H + X] = \sum_n d\sigma[A + B \rightarrow (Q\bar{Q})_n + X] \langle \mathcal{O}_n^H \rangle. \quad (7)$$

The sum over n includes the color, spin, and orbital-angular-momentum states of the $Q\bar{Q}$ pair. The pQCD cross sections are essentially inclusive *partonic cross sections* for creating the $Q\bar{Q}$ pair, which can be expanded in powers of $\alpha_s(m_Q)$, convolved with *parton distributions* for the colliding hadrons A and B . The NRQCD matrix element $\langle \mathcal{O}_n^H \rangle$ is essentially the probability for a $Q\bar{Q}$ pair created in the state n to evolve into a final state that includes the quarkonium H . It is a nonperturbative constant that scales with a definite power of the typical relative velocity v of the $Q\bar{Q}$ pair in H . It can be expressed as the vacuum

expectation value of a four-fermion operator in NRQCD [12]. The operators in color-singlet matrix elements are local operators, but those in color-octet matrix elements include Wilson lines [14]. The color-singlet matrix element that is leading order in v can be determined phenomenologically from an electromagnetic annihilation decay rate. The color-octet matrix elements can only be determined phenomenologically from measurements of quarkonium production.

Since the NRQCD matrix elements $\langle \mathcal{O}_n^H \rangle$ scale with definite powers of v that depend on n , the sum over n in Eq. 7 can be interpreted as an expansion in powers of v . The predictive power of NRQCD factorization comes from truncating that expansion. The truncation in v is more accurate for bottomonium than for charmonium, since v^2 is smaller by a factor of about 1/3. Since the relative velocity of the $Q\bar{Q}$ pair in an excited quarkonium state is not as small as in the ground state, the v expansion of NRQCD may converge more slowly for the excited states. Thus the truncation in v may introduce larger errors for $\psi(2S)$ than for J/ψ . By truncating in v and using approximate symmetries of NRQCD, the number of nonperturbative constants can be reduced to just a few for each orbital-angular-momentum multiplet of quarkonium. For a spin-triplet S -wave quarkonium state H , such as the J/ψ or the $\Upsilon(1S)$, the leading NRQCD matrix element is a color-singlet matrix element of order v^3 denoted by $\langle \mathcal{O}^H(^3S_1^{[1]}) \rangle$. It can be determined phenomenologically from the decay rate of H into a lepton pair. The truncation for S -wave states that is used in current phenomenology includes the NRQCD matrix elements through relative order v^4 . There are three independent color-octet matrix elements denoted by $\langle \mathcal{O}^H(^1S_0^{[8]}) \rangle$, $\langle \mathcal{O}^H(^3S_1^{[8]}) \rangle$, and $\langle \mathcal{O}^H(^3P_0^{[8]}) \rangle$, which are suppressed by orders v^3 , v^4 , and v^4 , respectively. The symbols in parentheses indicate the angular-momentum state $^{2S+1}L_J$ of the $Q\bar{Q}$ pair and whether its color state is singlet [1] or octet [8]. The truncation of the velocity expansion of NRQCD could be extended to a higher order in v only at the expense of introducing several additional phenomenological parameters.

When $p_T > m_Q$, the NRQCD factorization formula can be expanded in powers of m_Q/p_T . In the production of a spin-triplet S -wave quarkonium state, the cross sections in the various NRQCD channels have different behaviors at large p_T . At LO (leading order) in α_s , which is order $\alpha_s^3(m_Q)$, the only channel at LP (leading power) is $^3S_1^{[8]}$. The other color-octet channels $^1S_0^{[8]}$ and $^3P_0^{[8]}$ are NLP, and the color-singlet channel $^3S_1^{[1]}$ is N²LP. At NLO in α_s , all three color-octet channels are LP, while the color-singlet channel is NLP. The suppression of the color-singlet channel by powers of α_s and m_Q/p_T makes the color-octet channels important, despite their suppression by powers of v .

The NRQCD factorization formula is predictive of the quarkonium polarization. With the truncation for S -waves at relative order v^4 , the polarization is determined by the same four NRQCD matrix elements as the cross sections summed over quarkonium spins. In principle, measurements of hadroproduction cross sections summed over quarkonium spins could be used to determine the matrix elements and then predict the polarization. However, the $^1S_0^{[8]}$ and $^3P_0^{[8]}$ terms in the hadroproduction cross sections have similar dependence on kinematical variables, such as p_T . Thus, to determine them separately, one must in practice either use data from other production processes or else use polarization data.

2. LP Fragmentation Formula

The LP fragmentation formula is a rigorous factorization formula in which nonperturbative effects associated with the binding of a $Q\bar{Q}$ pair into quarkonium are organized into functions, instead of multiplicative constants as in Eq. 7. It states that the leading power (LP) of m_Q/p_T in the cross section for producing quarkonium at large p_T can be expressed as a sum of inclusive pQCD cross sections for producing a parton convolved with *fragmentation functions*:

$$d\sigma[A + B \rightarrow H + X] = \sum_i d\hat{\sigma}[A + B \rightarrow i + X] \otimes D_{i \rightarrow H}(z). \quad (8)$$

The sum over i extends over the types of partons (gluons, quarks, and antiquarks). The momentum of the parton i is determined by the condition that the quarkonium H has longitudinal momentum fraction z relative to the parton. The “ \otimes ” in Eq. 8 represents an integral over z . The pQCD cross sections are essentially inclusive partonic cross sections for producing the parton i , which can be expanded in powers of $\alpha_s(p_T)$, convolved with parton distributions for the colliding hadrons A and B . The fragmentation function $D_{i \rightarrow H}(z)$ is the nonperturbative probability distribution for the momentum fraction z . The evolution equations for the fragmentation functions can be used to sum large logarithms of p_T/m_Q to all orders in α_s . A proof of the LP factorization formula in Eq. (8) was first sketched by Nayak, Qiu, and Sterman in 2005 [15].

The LP fragmentation formula lacks the predictive power of the NRQCD factorization formula, because the fragmentation functions $D_{i \rightarrow H}(z)$ are nonperturbative functions of z that must be determined phenomenologically. Predictive power can be achieved by applying the NRQCD factorization conjecture to the fragmentation functions. It states that the fragmentation function for the parton i to produce the quarkonium H can be expressed as a sum of pQCD fragmentation functions multiplied by NRQCD matrix elements:

$$D_{i \rightarrow H}(z) = \sum_n d_{i \rightarrow (Q\bar{Q})_n}(z) \langle \mathcal{O}_n^H \rangle. \quad (9)$$

The pQCD fragmentation functions $d_{i \rightarrow (Q\bar{Q})_n}(z)$ can be expanded in powers of $\alpha_s(m_Q)$. The NRQCD-expanded LP fragmentation formula obtained by inserting Eq. 9 into Eq. 8 should reproduce the leading power in the expansion of the NRQCD factorization cross section in Eq. 7 in powers of m_Q/p_T . The LP factorization formula was actually first applied to quarkonium production at large p_T back in 1993, when the first fragmentation functions for quarkonium were calculated to LO in α_s [16, 17]. The fragmentation functions have since been calculated to NLO for all the phenomenologically relevant channels and to NLO for the ${}^3S_1^{[8]}$ channel [18]. The usefulness of the NRQCD-expanded LP fragmentation formula has proved to be limited. Explicit calculations using the NRQCD factorization formula have revealed that, in some channels, the LP cross section is not the largest contribution until p_T is almost an order of magnitude larger than m_Q .

In the NRQCD-expanded LP fragmentation formula, there are three expansion parameters: $\alpha_s(p_T)$, $\alpha_s(m_Q)$, and v . The various NRQCD channels enter at different orders in $\alpha_s(m_Q)$. For spin-triplet S -wave quarkonium, the only channel that is LO in α_s is ${}^3S_1^{[8]}$ at order $\alpha_s^2(p_T)\alpha_s(m_Q)$. The other color-octet channels ${}^1S_0^{[8]}$ and ${}^3P_0^{[8]}$ are NLO at order $\alpha_s^2(p_T)\alpha_s^2(m_Q)$. The color-singlet channel ${}^3S_1^{[1]}$ is N²LO at order $\alpha_s^2(p_T)\alpha_s^3(m_Q)$. The suppression of the color-singlet channel by powers of $\alpha_s(m_Q)$ makes the color-octet channels important, despite their suppression by powers of v .

The NRQCD-expanded LP fragmentation formula has important implications for the polarization of spin-triplet S -wave quarkonium at large p_T . The contribution that is LO in $\alpha_s(p_T)$ comes from production of a hard gluon. At LO in $\alpha_s(m_c)$, that gluon fragments into a $Q\bar{Q}$ pair in the ${}^3S_1^{[8]}$ channel [19]. The gluon is transversely polarized in the cm-helicity frame, and at leading order in v , that polarization is transferred to the quarkonium. Thus, at asymptotically large p_T , spin-triplet S -wave quarkonium should be increasingly transversely polarized [20].

3. NLP Fragmentation Formula

The NLP fragmentation formula is a rigorous extension of the LP fragmentation formula in Eq. 8 to the next-to-leading power (NLP) of m_Q^2/p_T^2 . Kang, Qiu, and Sterman proved in 2011 that the terms suppressed by m_Q^2/p_T^2 can be written as a sum of pQCD cross sections for producing a collinear $Q\bar{Q}$ pair convolved with *double-parton fragmentation functions* [21, 22]:

$$\sum_n d\hat{\sigma}[A + B \rightarrow (Q\bar{Q})_n + X] \otimes D_{(Q\bar{Q})_n \rightarrow H}(z, \zeta, \zeta'). \quad (10)$$

The sum over n extends over the color (singlet and octet) and Lorentz (vector, axial-vector, and tensor) structures of the $Q\bar{Q}$ pair. The pQCD cross sections are essentially inclusive partonic cross sections for producing a collinear $Q\bar{Q}$ pair, which can be expanded in powers of $\alpha_s(p_T)$, convolved with parton distributions for the colliding hadrons A and B . The double-parton fragmentation functions $D_{(Q\bar{Q})_n \rightarrow H}(z, \zeta, \zeta')$ are nonperturbative probability distributions in the longitudinal momentum fraction z of the quarkonium H relative to the $Q\bar{Q}$ pair that also depend on the relative longitudinal momentum fractions ζ and ζ' of the Q and the \bar{Q} . The “ \otimes ” in Eq. 8 represents integrals over z , ζ , and ζ' . The NLP fragmentation formula is obtained by adding Eq. (10) to Eq. (8). The evolution equations for the fragmentation functions can be used to sum large logarithms of p_T/m_Q to all orders in α_s . A similar factorization formula has been derived by Fleming *et al.* using soft collinear effective theory [23, 24], but it is not identical. In particular, the form of the evolution equations for the fragmentation functions is different in the two approaches.

The NLP fragmentation formula lacks predictive power, because the double-parton fragmentation functions are nonperturbative functions of z , ζ , and ζ' that must be determined phenomenologically. Predictive power can be achieved by applying the NRQCD factorization conjecture to the fragmentation functions. The double-parton fragmentation functions $D_{(Q\bar{Q})_n \rightarrow H}(z, \zeta, \zeta')$ have expansions in terms of the NRQCD matrix elements analogous to that for the single-parton fragmentation function $D_{i \rightarrow H}(z)$ in Eq. 9 [25, 26]. The NRQCD-expanded NLP fragmentation formula should reproduce the power expansion of the NRQCD factorization cross section in Eq. 7 up to order m_Q^2/p_T^2 .

Kang, Qiu, and Sterman have taken the first step towards analyzing the effects of $Q\bar{Q}$ fragmentation on the polarization of quarkonium [22]. For a spin-triplet S -wave quarkonium state, the only $Q\bar{Q}$ fragmentation function that is nonzero at LO in α_s is the color-octet axial-vector fragmentation function. Its contribution to the cross section is increasingly longitudinal in the cm-helicity frame as p_T increases. They argued that the observed polarization of quarkonium could arise from a competition between a transversely polarized contribution from gluon fragmentation and a longitudinally polarized contribution from $Q\bar{Q}$ fragmentation. At very large p_T , the leading power correction to the polarization comes

from interference between gluon fragmentation and $Q\bar{Q}$ fragmentation, and it falls like a single power of m_Q/p_T [27]. Thus NLP factorization predicts that the polarization at large p_T should eventually be increasingly transverse, as predicted by LP factorization, but this asymptotic behavior may not appear until very large p_T .

4. Color-Singlet Model

One of the earliest attempts to describe quarkonium production using perturbative QCD was the *color-singlet model* [28–31]. A $Q\bar{Q}$ pair that is created in a high energy collision is assumed to be able to bind to form a quarkonium H only if it is created in a color-singlet state and in the same spin and orbital-angular-momentum state as the $Q\bar{Q}$ pair in H . The color-singlet model can be obtained from the NRQCD factorization formula by assuming that the only nonzero NRQCD matrix element is the color-singlet matrix element that is leading order in v . For a spin-triplet S -wave state H , such as the J/ψ or the $\Upsilon(1S)$, that matrix element is $\langle \mathcal{O}^H(^3S_1^{[1]}) \rangle$. Since this matrix element is determined by the decay rate of H into a lepton pair, the color-singlet model has no adjustable parameters. In the case of P -wave states, the color-singlet model is inconsistent, because of infrared divergences at low orders in α_s .

The color-singlet model gives unambiguous predictions for the polarization of spin-triplet S -wave quarkonium. The predictions at LO and NLO in α_s are completely different [32–35]. At LO, the polarization in the cm-helicity frame is strongly transverse, with λ_θ approaching 1 as p_T increases, while the polarization in the CS frame is weakly longitudinal and varies slowly with p_T . At NLO, the polarization in the cm-helicity frame is increasingly longitudinal as p_T increases, while the polarization in the CS frame is transverse and varies slowly with p_T .

5. Color-Evaporation Model

The earliest attempt to describe quarkonium production using perturbative QCD was the *color-evaporation model* [36, 37]. A $Q\bar{Q}$ pair that is created in a high energy collision of hadrons is assumed to be able to bind to form the quarkonium H only if its invariant mass is below the open-heavy-flavor threshold. The probability f_H of binding is assumed to be independent of the color or spin state of the $Q\bar{Q}$ pair. If the $Q\bar{Q}$ phase space integrals are expanded around the threshold, the color-evaporation model reduces to the NRQCD factorization formula with simplifying assumptions about the NRQCD matrix elements [38].

The color-evaporation model, as originally conceived, predicts zero polarization for quarkonium states. In principle, the model could be extended to give nontrivial predictions for polarization by identifying the total spin of the Q and \bar{Q} with the spin of the quarkonium. Such an extension is not feasible in practice, because the cross sections in the color-evaporation model are calculated using NLO pQCD cross sections for producing Q and \bar{Q} in which their spin states have been summed over.

6. k_T Factorization

The k_T -factorization approach is an alternative to standard collinear factorization in which pQCD cross sections are expressed in terms of parton distributions that depend on the transverse momenta of the partons, as well as on their longitudinal momentum fractions. The k_T -factorization approach includes some contributions at leading order in α_s that would appear only at higher orders in collinear factorization. The k_T -dependent parton distributions are known phenomenologically with much less precision than the collinear parton distributions. The transverse momentum of the colliding partons is not expected to be important at large p_T .

In the applications of k_T factorization to quarkonium production, production is usually assumed to occur only through the color-singlet $Q\bar{Q}$ channel that is leading order in v and the pQCD cross sections are usually calculated only to LO in α_s . In this approximation, the polarization of the $\Upsilon(1S)$ in the cm-helicity frame is predicted to be increasingly longitudinal as p_T increases [39, 40].

C. NRQCD Factorization Phenomenology

In order to use NRQCD factorization to predict the polarization of quarkonium, the color-octet NRQCD matrix elements must be determined phenomenologically. Early predictions of the polarization were based on fits using pQCD cross sections calculated to LO [41–43]. Since then, three independent groups have carried out the heroic calculations of all the relevant pQCD cross sections to NLO [44–46]. Recent predictions of quarkonium polarization have been based on fits of the color-octet matrix elements using NLO pQCD cross sections.

In order to predict the polarization, it is essential to take into account the feeddown from the direct production of higher quarkonium states. The prompt production rate for J/ψ includes significant feeddown from the direct production of $\psi(2S)$ and $\chi_{cJ}(1P)$. The prompt production rate for $\Upsilon(1S)$ includes significant feeddown from the direct production of $\Upsilon(2S)$, $\Upsilon(3S)$, $\chi_{bJ}(1P)$, and $\chi_{bJ}(2P)$. The feeddown contributions to the unpolarized cross sections for J/ψ and $\Upsilon(1S)$ are about 30 or 40%. However, the feeddown contributions could have a larger effect on the polarization.

NRQCD predictions for the polarization of the J/ψ vary dramatically, depending on the data used to determine the color-octet NRQCD matrix elements. All of the groups include the data from CDF Run II for $d\sigma/dp_T$ with p_T greater than 7 GeV. A prediction of strong transverse polarization in the cm-helicity frame [34] arises if one includes in the fits the HERA data for photoproduction of J/ψ down to a p_T of 3 GeV. A prediction of moderate transverse polarization [46] arises if one includes in the fits the data from LHCb for $d\sigma/dp_T$ with p_T greater than 7 GeV and if one uses NRQCD factorization predictions to correct for feeddown from the $\psi(2S)$ and the χ_{cJ} states. A prediction of near-zero transverse polarization [47] arises if one includes in the fits the CDF Run II polarization measurement.

A complete NLO NRQCD analysis of the $\Upsilon(nS)$ states, including the effects of feeddown, has recently been carried out [48]. The color-octet matrix elements for the S -wave and P -wave states were determined by fitting cross sections and polarization data measured at the Tevatron and the LHC with $p_T > 8$ GeV. The $\Upsilon(1S)$ and $\Upsilon(2S)$ states are predicted to have small transverse polarizations in the cm-helicity frame. The $\Upsilon(3S)$ is predicted to have a more rapidly increasing transverse polarization as p_T increases. The difference might not be as dramatic if feeddown from the $\chi_{bJ}(3P)$ were taken into account.

IV. EXPERIMENTAL ISSUES FOR POLARIZATION MEASUREMENTS

Hadronic production processes for quarkonium states contain two *prompt* contributions in which the quarkonium is produced at the hadronic collision point:

- (a) *direct* production, in which the quarkonium is produced by the binding of a heavy quark and antiquark created by the strong interactions of QCD,
- (b) *feeddown*, in which the quarkonium is produced by hadronic or electromagnetic transitions from a higher state in the quarkonium spectrum that was produced directly.

At large center-of-mass energy \sqrt{s} , B -hadron decays produce additional charmonium events that are removed by comparing the location of the dilepton vertex with that of the primary vertex where the hadrons collided.

For the spin-triplet S -wave states of interest, feeddown events come from decays of higher radial excitations and orbital-angular-momentum excitations. This can modify both the polarization and the kinematic variables of the lower-mass S -wave state compared to its direct production properties. The photons and pions from the feeddown transitions have low energy. In a hadronic production environment, it is difficult to measure such low-energy tracks and to associate them correctly with the dimuon pair in order to separate feeddown and direct production.

The material for the bulk of this review originates from experiments done with $p\bar{p}$ collisions at 1.8 and 1.96 TeV center-of-mass energy at the Fermilab Tevatron and with pp collisions at 7 TeV center-of-mass energy at the Large Hadron Collider (LHC) at CERN. Other studies at lower \sqrt{s} , including J/ψ and Υ polarization studies in pA collisions by the E866 (NuSea) Collaboration at Fermilab, J/ψ polarization measurements in pA collisions by the HERA-B Collaboration at DESY, and J/ψ polarization measurements in pp collisions by the PHENIX Collaboration at Brookhaven, contribute results at smaller p_T .

Measuring quarkonium polarization puts stringent requirements on experiment design and apparatus performance. Polarization is a differential measurement; it uses the lab frame trajectories of two leptons to determine the decay momentum vector of ℓ^+ with respect to a quantization axis in the dilepton rest frame. For polarization, not only must one know the apparatus efficiency for all events within the acceptance coverage, but also the acceptance must cover a large fraction of the decay angular variables in order to determine the three polarization parameters λ_θ , λ_ϕ , and $\lambda_{\theta\phi}$ that describe the decay process (Eq. 1). In polarization experiments, the more complete the angular phase space coverage, the better the determination of the polarization parameters. Until recently, quarkonium polarization measurements have focussed on just the single parameter λ_θ for a specific spin-quantization axis. Modern experiments, prompted by the discussions in Ref. [2, 5], have moved to measure all three polarization parameters in several reference frames in their analyses. One important advantage is that this allows the frame-invariant polarization parameters $\tilde{\lambda}$ and $\tilde{\lambda}'$ defined in Sec. II to be used as diagnostics for possible inconsistencies.

A. Background Determination and Angular Characteristics

Polarization experiments are sensitive to the angular structure of the background in the dilepton rest frame. Demonstrating good control of the background angular distribution

is essential for any polarization experiment. In almost all experiments, the background definition procedure is the same:

1. make a dilepton mass plot of selected prompt or (for charmonium only) B -decay events in each analysis phase space bin ($\Delta p_T, \Delta x_F$ or $\Delta y, \Delta \cos \theta$);
2. fit the sideband background to a suitable empirical function and the signal shape to a predetermined functional form, often based on simulation;
3. either subtract the estimated background to determine the signal yield and uncertainty in that phase space bin or, when sample sizes are large, make a simultaneous fit to signal distributions and background distributions to maximize the statistical power.

For experiments that analyze the two-dimensional decay angular distribution, the phase space becomes four-dimensional; binning in the azimuthal angle ϕ is also required, and the mass plot is done in $\cos \theta - \phi$ space for each bin of p_T and the longitudinal variable.

B. Apparatus Acceptance

Every polarization measurement must determine the apparatus acceptance after all the kinematic selections on the individual leptons have been applied and also must determine the efficiency for triggering on and detecting each of the leptons that falls into the acceptance. Simulation techniques are primary tools for these studies, but experimental validation of the Monte Carlo results is highly desirable. Using GEANT-based simulation models [49] makes the acceptance calculations robust. Single-lepton kinematic distributions for data and Monte Carlo samples are compared to validate the quarkonium kinematic parameters of the simulation. Two different approaches are used:

- (a) generate *only* quarkonium events using an event generator, typically EvtGen [50], that specifies the laboratory frame kinematics (p_T and x_F or $|y|$ distributions) of the quarkonium based on other measurements, perhaps by the same group,
- (b) use a complete event generator like Pythia [51] to generate the quarkonium states inclusively, with kinematic distributions chosen by Pythia or possibly adjusted for the experiment.

In order to use option (a), the experiment has to have a tracking detector with low average occupancy, so that lepton track reconstruction is unlikely to be distorted by the presence of other tracks in the event. For option (b) with Pythia generation, the simulation procedure generates the quarkonium kinematics and also produces the decay. If reweighting has to be done to match kinematic parameters, it occurs *ex post facto*, and there can be distortion of the generated event distribution in the quarkonium rest frame due to reweighting. The quantization axis of the generated event is not the same as the corresponding quantity after reweighting. Of course, the extent of any such shift can be studied and its impact on the polarization parameters evaluated within the Monte Carlo framework.

The lepton detection efficiency can vary with the kinematic variables of the lepton ℓ , usually its transverse momentum $p_T(\ell)$ with respect to the beam direction and its pseudorapidity $\eta(\ell) = -\ln[\tan(\theta/2)]$. The tag-and-probe method of efficiency determination is used in most modern experiments [52]. The *probe* track, unbiased by a trigger, is either

passed or failed by the analysis criteria. Probe track efficiencies in (p_T, η) bins can give the distribution of the trigger and detection efficiency for a single track as a function of its kinematic parameters. The tag-and-probe method can also be applied to Monte Carlo samples with large statistics. If the simulation and data efficiency distributions agree, then one can use the Monte Carlo shape to fit to the data in order to improve knowledge of the kinematic variation of efficiencies. In some experiments, tag-and-probe studies are not possible, so simulation studies provide both efficiency and acceptance. This introduces a level of uncertainty into the results that can be hard to quantify.

V. EXPERIMENTS AND RESULTS

The general procedures outlined in the previous section have been used both in fixed target experiments (using proton or pion beams) and in collider experiments at the Tevatron ($p\bar{p}$ collisions) and at Fermilab, RHIC or LHC (pp or pA collisions). We focus here on the experiments that have produced the highest statistics measurements for charmonium and bottomonium polarization in each class of experiments.

A. Fixed Target Experiments

Two very different fixed target experiments dominate the field: Fermilab E866 (NuSea) [53, 54] at $\sqrt{s} = 38.8$ GeV and HERA-B [55] at $\sqrt{s} = 41.6$ GeV. Both use nuclear targets. At these center-of-mass energies, $\psi(2S)$ production and non-prompt J/ψ production are negligible. The transverse momentum p_T is, at best, comparable to the charmonium mass. Because these are well-discussed experiments, we only summarize their results. For NuSea, the polarization parameter λ_θ in the Collins-Soper (CS) frame for J/ψ polarization is small over the p_T range < 4 GeV, with an average of $+0.15$ for $\langle x_F \rangle = 0.45$. For HERA-B, the effective λ_θ parameter in the CS frame is negative, averaging to -0.18 for $\langle x_F \rangle = -0.12$. This may indicate sensitivity of the polarization to the production x_F range at low p_T in pA collisions. The HERA-B results confirm that the three polarization parameters are all small, both in the cm-helicity and CS frames.

The NuSea Υ analysis finds that the combined system for $\Upsilon(2S)$ and $\Upsilon(3S)$ has a polarization very similar to that of Drell-Yan dimuon pairs in the Collins-Soper frame [56], fully transversely polarized for $p_T < 4$ GeV for $\langle x_F \rangle \sim 0.23$. In contrast, the $\Upsilon(1S)$ λ_θ parameter is essentially zero for $p_T < 1.8$ GeV.

B. Tevatron Polarization Measurements

At collider energies, one has to consider both prompt and decay sources for charmonium. For colliding beams, x_F will always be small because p_{\max} is large. The appropriate kinematic variables for quarkonium are transverse momentum p_T and rapidity y . The first Tevatron collider measurements were made in the central region $|y| < 0.6$ with $p_T < 20$ GeV. The CDF collaboration reported that the fraction of J/ψ mesons that came from χ_c feeddown was $0.45 \pm 0.05 \pm 0.15$ for $p_T > 6$ GeV, $|y| < 0.5$ [57]. The D0 collaboration reported that this feeddown fraction was $0.35 \pm 0.07 \pm 0.07$ for $p_T > 8$ GeV, $|y| < 0.6$ [58]. For bottomonium, CDF [59] determined that the fraction of directly-produced $\Upsilon(1S)$ mesons

having $p_T > 8$ GeV is $0.509 \pm 0.082 \pm 0.090$, very similar (the same within uncertainties) to the J/ψ result. The feeddown fraction in quarkonium production seems to be at most mildly dependent on beam energy, p_T range, target type, and which heavy quark is involved. We will want to look at polarization systematics in this light.

In Run 1 of the Tevatron, CDF made measurements of J/ψ , $\psi(2S)$, and $\Upsilon(1S)$ polarization at $\sqrt{s} = 1.8$ TeV. In Run 2 of the Tevatron, \sqrt{s} was increased to 1.96 TeV and the integrated luminosity increased by more than an order of magnitude. Both CDF and D0 made measurements of bottomonium polarization, and CDF repeated its study of J/ψ and $\psi(2S)$ polarization.

1. Quarkonium Polarization at $\sqrt{s} = 1.8$ TeV

The CDF polarization measurements in the cm-helicity frame from Run 1 are well known [52]. We note that in this pioneering experiment, covering a rapidity range $|y| < 0.6$, only 60% of the detected muons were measured in the vertex detector. This makes the determination of the efficiency more difficult for asymmetric decays compared to later experiments that had full coverage. For prompt J/ψ events, the average $\langle \lambda_\theta \rangle = +0.21 \pm 0.05$ and all measurements were positive for the range $p_T < 15$ GeV. However, there was no suggestion that the polarization was becoming more transverse as p_T increased. The $\psi(2S)$ polarization was measured, but had large uncertainties.

For the $\Upsilon(nS)$ states, the yields of the higher excited states were low, and only the $\Upsilon(1S)$ polarization is reported [60]. The rapidity range was $|y| < 0.4$, so that the acceptance of the vertex detector was somewhat larger than for the J/ψ case. The polarization parameter λ_θ in the cm-helicity frame was measured in four p_T bins. All are consistent with zero within one standard deviation, with $\langle \lambda_\theta \rangle = -0.12 \pm 0.22$.

2. D0 Run 2 $\Upsilon(nS)$ Polarization

The D0 Collaboration measured the $\Upsilon(nS)$ polarization in the cm-helicity frame [61]. The dataset covered a large rapidity range, $|y| < 1.8$. High rapidity events have poorer mass resolution than central events, and the three $\Upsilon(nS)$ states overlapped in the mass distribution. The D0 analysis imposed a muon isolation cut to purify the sample. This has not been done in any other polarization experiment. Unlike other experiments, there is a very small sideband region on the low mass side of the $\Upsilon(1S)$ signal region due to a combination of poor mass resolution and a dimuon trigger threshold. The background shape under the broad signal region is poorly constrained by the data.

The D0 simulation uses Pythia to study unpolarized $\Upsilon(1S)$ (or $\Upsilon(2S)$) decays to two muons. The dimuon p_T distribution and the total momentum from the Monte Carlo were reweighted to match the data. This influences the helicity boost and a systematic uncertainty is assigned. After corrections, the simulated $\Upsilon(1S)$ mass peak is 40 MeV different from the PDG value. This is a much larger discrepancy than is seen in the simulations from other experiments. The measured λ_θ parameter as a function of p_T for the $\Upsilon(1S)$ in the range $|y| < 1.8$ is very different from what was reported by CDF in the Run 1 measurement for a similar p_T range but covering only the central rapidity region $|y| < 0.4$. For $p_T < 10$ GeV, $\langle \lambda_\theta \rangle = -0.45 \pm 0.06$.

3. CDF Run 2 Charmonium Polarization

The CDF Run 2 J/ψ and $\psi(2S)$ polarization measurements were done in the cm-helicity frame for $|y| < 0.6$ [62]. All tracks with $\eta < 0.6$ traversed the silicon vertex detector, improving the efficiency compared to Run 1. The analysis followed the same methodology as the Run 1 measurement. A simultaneous fit to the dimuon mass and the transverse vertex position separated events into prompt and B -hadron decay candidates. Muon efficiencies and trigger efficiencies were determined by experimental tag-and-probe studies for all three trigger levels. These efficiencies were applied to simulated muons in fully polarized (T or L) Monte Carlo samples in order to account for apparatus effects.

The average λ_θ parameter in the cm-helicity frame for the J/ψ from this analysis is small and consistently negative $\langle \lambda_\theta \rangle = -0.062 \pm 0.013$. This disagrees with the CDF Run 1 result. On the other hand, the B -hadron decay polarization for the Run 2 data gives an effective $\lambda_\theta^B = -0.11 \pm 0.04$, consistent both with the Run 1 result and with the Monte Carlo simulation of $B \rightarrow J/\psi X$ decays. Large statistical uncertainties preclude any statement about the $\psi(2S)$ polarization.

4. CDF Run 2 Bottomonium Polarization

The CDF Run 2 study of $\Upsilon(nS)$ polarization [63] for a rapidity range $|y| < 0.6$ introduced new analysis steps to improve background control and yielded several first-time results. This study, with better statistical accuracy than any other measurement, is the first to make a simultaneous determination of the three polarization parameters for the two-dimensional $(\cos\theta, \phi)$ distribution using the methods discussed in Sec. II. It also produced the first measurement of the $\Upsilon(3S)$ polarization parameters. The trigger efficiency and single-muon efficiencies were evaluated using tag-and-probe analyses for all three dimuon trigger levels. The acceptance was determined from unpolarized Monte Carlo simulations.

The analysis for the three polarization parameters λ_θ , λ_ϕ , and $\lambda_{\theta\phi}$ for each mass peak was done following the outline in Sec. II. It covers the range $2 < p_T < 40$ GeV. The data were separated into p_T bins. In each bin, the data were boosted to the cm-helicity or CS analysis frame and the angular variables $(\cos\theta, \phi)$ were divided into $0.05 \times 5^\circ$ bins. Ref. [63] gives the details of how the displaced sample background was used to constrain the background in the signal region by a series of fits. Independent fits were done in the cm-helicity frame and the CS frame and their consistency is validated using the frame-invariant polarization parameter $\tilde{\lambda}$. There is no indication that there is any high- p_T change in the polarization for any of the three states. These are the most precise determinations of the $\Upsilon(nS)$ now available. For the $\Upsilon(1S)$ in the cm-helicity frame, $\langle \lambda_\theta \rangle = -0.102 \pm 0.027$ for $p_T < 12$ GeV, agreeing with CDF Run 1 and disagreeing with D0.

C. RHIC and LHC Polarization Studies

The advent of pp colliders allowed quarkonium studies with targets similar to the fixed target studies, but in a very different kinematic regime. PHENIX at RHIC and ALICE, CMS, and LHCb at LHC have published J/ψ polarization studies and CMS has published results on $\Upsilon(nS)$ polarizations. The ALICE results are dominated by those of LHCb, which covers the kinematic range $2 < p_T < 15$ GeV and forward rapidity $2 < y < 4.5$. The

CMS results cover the high- p_T (14-70 GeV), central rapidity ($|y| < 1.2$) regime. All three experiments present results in both the cm-helicity and CS frames. The random dimuon background for the quarkonium states is much lower at the LHC than for the Tevatron. This simplifies the background subtraction.

1. CMS Bottomonium Polarization

Polarization results for all three $\Upsilon(nS)$ states having $10 < p_T < 50$ GeV and two rapidity ranges for $|y| < 1.2$ are reported by CMS in Ref. [64]. The offline minimum p_T requirement was 10 GeV to ensure stable efficiency measurements. The single-muon trigger efficiencies were based on tag-and-probe studies.

The analysis grouped dimuon events in p_T bins for $|y| < 0.6$ or $0.6 < |y| < 1.2$. The CMS measurement, like the CDF study, shows that all three polarization parameters are small for all three Υ states, both in the cm-helicity and the CS frames. The frame-invariant variable $\tilde{\lambda}$ for each state indicates good agreement between frames, compatible with the range of variation expected from simulation studies. The $\Upsilon(3S)$ polarization parameters do not rise at large p_T . For the $\Upsilon(1S)$ in the cm-helicity frame, $\langle \lambda_\theta \rangle = +0.074 \pm 0.064$ for the range $10 < p_T < 30$ GeV for pp .

2. CMS Charmonium Polarization

The CMS Collaboration used the same analysis technique to determine the polarization parameters of charmonium [65]. This data set has the largest reported sample of J/ψ mesons used for polarization analysis and provides the first meaningful polarization measurements for the $\psi(2S)$. For the J/ψ , results are reported for $14 < p_T < 70$ GeV in two rapidity ranges: $|y| < 0.6$ and $0.6 < |y| < 1.2$. For the $\psi(2S)$, the phase space covered was $14 < p_T < 50$ GeV in three rapidity ranges: $|y| < 0.6$, $0.6 < |y| < 1.2$, and $1.2 < |y| < 1.5$.

Events were separated into prompt and B -hadron decay candidates by making a fit to the transverse vertex displacement from the primary. There are no large polarization parameters in either the cm-helicity or CS frame, and the $\tilde{\lambda}$ test shows good consistency for the analysis. Detailed results will be discussed below.

3. LHCb and ALICE Charmonium Polarization

These two experiments report J/ψ polarization parameters at forward rapidity in the cm-helicity and CS frames. In ALICE [66], a muon spectrometer gave forward coverage with modest mass resolution. Contributions from $\psi(2S)$ were ignored. Polarization variables λ_θ and λ_ϕ were determined from the dimuon mass spectrum binned in $\cos \theta$ or ϕ . The sidebands are used to subtract the background under the J/ψ mass peak in each projected angle bin. The resulting experimental distributions were corrected for efficiency and for acceptance using simulated events from an unpolarized Monte Carlo study.

The LHCb [67] coverage was $2 < p_T < 15$ GeV for $2 < y < 4.5$ with good mass resolution. The LHCb analysis also relies on simulation to determine efficiency and acceptance, but they have a major advantage in calibrating the results – a sample of fully-reconstructed $B^+ \rightarrow J/\psi K^+$ decays for which the J/ψ polarization is known. The LHCb mass distribution for J/ψ events has very little background. The usual subtraction technique is used.

Both LHCb and ALICE observe small polarization in this p_T range, and the other two polarization parameters (just λ_ϕ for ALICE) are consistent with being zero in the cm-helicity frame throughout this p_T range. The ALICE analysis finds $\langle\lambda_\theta\rangle = -0.14\pm 0.10$. The average λ_θ parameter from LHCb is -0.063 ± 0.011 for the range $2 < p_T < 15$ GeV. Overall the LHCb polarization parameter measurements in either frame show little variation with y or p_T within their joint ranges.

4. PHENIX Charmonium Polarization

The PHENIX Collaboration at RHIC identified J/ψ events in the e^+e^- channel from 200 GeV pp collisions with $|y| < 0.35$ and $p_T(ee) < 5$ GeV. [68]. Electron efficiencies from simulation were calibrated using photon conversion electrons from the beam pipe and unpolarized simulated decays were used to correct the data and determine λ_θ in the cm-helicity and Gottfried-Jackson (GJ) frames. The PHENIX pp phase space for $\sqrt{s}=200$ GeV is similar to that for the HERA-B pA measurement at $\sqrt{s}=41.6$ GeV, and the PHENIX polarization results agree with the more precise HERA-B measurements.

D. Experimental Summary

What can we conclude from the variety of experimental results presented here? We choose to present the measurements in two ranges: $p_T < 10$ GeV and $p_T > 10$ GeV. This choice reflects both the experimental information and the p_T behavior of the quarkonium production cross sections. Roughly independent of target and \sqrt{s} , the differential cross section peaks near $p_T \sim 2$ GeV (4 GeV) for J/ψ ($\Upsilon(1S)$) production. For $p_T > 10$ GeV it falls smoothly for both states. The low p_T range has data from collider and fixed target experiments. The large p_T range is covered only by collider experiments. A first question to consider is how much does \sqrt{s} matter in polarization results at low p_T . The experiments cover the range 38.8 GeV $< \sqrt{s} < 7$ TeV for pA collisions, $p\bar{p}$ collisions, and pp collisions at both low and high rapidity.

1. Polarization Results for J/ψ with $p_T < 10$ GeV

In general, the J/ψ polarization measurements in the cm-helicity or CS frames vary somewhat among experiments, but the polarization parameters are never large. The contributing experiments are HERA-B with pA collisions, ALICE, LHCb and PHENIX with pp collisions, and CDF Run 1 and Run 2 with $p\bar{p}$ collisions. Of these, ALICE and LHCb are large rapidity measurements; the others are central.

The λ_θ parameter in the cm-helicity frame for the six experiments is plotted versus p_T in Fig. 2. The HERA-B λ_θ measurement is nearly zero for $p_T > 1$ GeV. For PHENIX over the range $0 < p_T < 5$ GeV, $\langle\lambda_\theta\rangle = -0.10^{+0.05}_{-0.09} \pm 0.05$. The CDF Run 2 average is $\lambda_\theta = -0.035 \pm 0.016$ for $5 < p_T < 9$ GeV. The CDF Run 1 average $\langle\lambda_\theta\rangle = +0.21 \pm 0.05$ disagrees with CDF Run 2. At low p_T for J/ψ production, ALICE, CDF Run 2, HERA-B, LHCb, and PHENIX agree that λ_θ in the cm-helicity frame is negative and close to zero for p_T between 1 and 10 GeV independent of target, \sqrt{s} , or rapidity range. The CDF Run 1 result looks like an experimental outlier.

ALICE, CDF, HERA-B, LHCb, and PHENIX: J/ψ λ_θ vs p_T

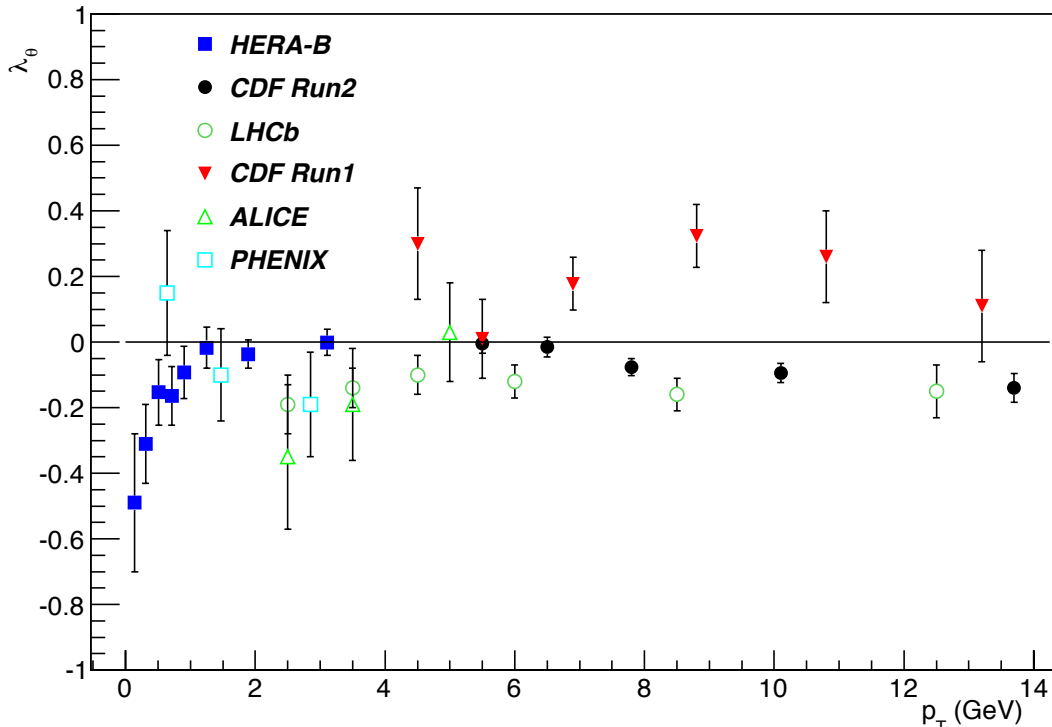


FIG. 2: Measurements of λ_θ in the cm-helicity frame for J/ψ production with $p_T < 10$ GeV. The data are from ALICE, CDF Run 1, CDF Run 2, HERA-B, LHCb, and PHENIX.

NuSea only reports data on λ_θ for forward x_F in the CS frame, assuming $\lambda_\phi = 0$. That assumption is consistent with ALICE and HERA-B and LHCb observations.

The overall picture shows that J/ψ polarization for $p_T < 10$ GeV is small for production from any kind of target, at any \sqrt{s} , and any rapidity in both the cm-helicity and CS frames. In this p_T range, no measurements of $\psi(2S)$ polarization give any useful limits.

2. Polarization Results for J/ψ and $\psi(2S)$ with $p_T > 10$ GeV

Data for $p_T > 10$ GeV come mostly from CMS measurements, which probe a new energy regime as well as extending the p_T region. Feeddown effects are a complication for interpreting J/ψ polarization results, so we look first at the $\psi(2S)$ results from CMS in the cm-helicity frame. For $|y| < 0.6$, the $\psi(2S)$ polarization parameters are consistent with being p_T -independent in the range $14 < p_T < 50$ GeV. The average λ_θ for the interval is 0.13 ± 0.12 , and gives no sign of becoming significantly transverse, even though uncertainties on individual points are not small. At higher rapidity, $0.6 < |y| < 1.2$, the trend is again for a p_T -independent λ_θ . In the cm-helicity frame, $\langle \lambda_\theta \rangle = -0.092 \pm 0.088$, which is more negative than for $|y| < 0.6$ but consistent to within 1.5 standard deviations. Polarization parameters for $\psi(2S)$ production are small both in the cm-helicity and CS frames and show little variation in the (p_T, y) phase space of the CMS measurement.

The J/ψ polarization from the CMS measurements again shows a stable p_T -independent

pattern over the range $14 < p_T < 70$ GeV in both rapidity ranges for the cm-helicity frame. Like the $\psi(2S)$ case, the p_T -averaged λ_θ value becomes slightly less positive at higher rapidity, with average values of 0.14 ± 0.04 at smaller rapidity and 0.08 ± 0.03 at larger rapidity, but consistent within 1.5 standard deviations. None of the three polarization parameters is large in either the cm-helicity or CS frame.

There is some tension between the LHCb results and the CMS results, even though there is no overlap in the data. The large-rapidity LHCb λ_θ results in the cm-helicity frame show a persistent negative polarization in the domain $p_T < 15$ GeV, $2 < y < 4.5$. The CMS measurements for $|y| < 1.2$ and $p_T > 14$ GeV are all positive. The uncertainties on the individual bin measurements near the boundary regions in (p_T, y) space are not small from either experiment, making it difficult to project a trend from one phase space region into the other. Future LHC measurements may clarify the issue.

3. Polarization Results for $\Upsilon(nS)$ with $p_T < 10$ GeV

Bottomonium polarization results at low p_T have been published by NuSea, CDF Run 1, CDF Run 2, and D0 Run 2. The NuSea results are in a different kinematic region from the other experiments and have no independent check. For $0 < x_F < 0.6$ and $p_T < 4$ GeV, the measured polarization in the CS frame from NuSea is transverse, like Drell-Yan polarization, for the two excited S-wave states $\Upsilon(2S) + \Upsilon(3S)$ compared to nearly zero polarization for the $\Upsilon(1S)$. Large polarization of any $\Upsilon(nS)$ state in the CS frame is not seen in high energy collider experiments. The pattern of the NuSea results is unusual.

The Tevatron experiments are summarized in Fig. 3, taken from Ref. [63]. For $p_T < 10$ GeV, the CDF Run 1 and CDF Run 2 results are statistically consistent, while the D0 measurement is radically different. Note that only the CDF Run 2 experiment has employed the $\tilde{\lambda}$ systematic uncertainty test to validate its results internally. The consistency of that test, the large statistical weight of the sample, and the independent confirmation from CDF Run 1 tends to argue that the D0 λ_θ results are outliers. The previous discussion of the D0 experiment noted that background subtraction was difficult because of the poor mass resolution and the limited background region on the low mass side of the signal region.

The CDF Run 2 data are the first good-statistics measurements of the $\Upsilon(2S)$ and $\Upsilon(3S)$ polarizations. None of the three polarization parameters for the higher-mass S-wave states shows any significant p_T structure in either the cm-helicity or CS frame for $p_T < 10$ GeV.

4. Polarization Results for $\Upsilon(nS)$ with $p_T > 10$ GeV

The p_T range for the CDF Run 2 measurements extends to 40 GeV. At the LHC, the CMS collaboration has measured $\Upsilon(nS)$ polarizations in the range $10 < p_T < 50$ GeV. We can compare the CMS measurements for $|y| < 0.6$ with the CDF Run 2 results to look for possible p versus \bar{p} target effects. We compare the λ_θ parameter in the cm-helicity frame for all three $\Upsilon(nS)$ states in Fig. 4. The general features of the two measurements show only a small p_T variation of λ_θ for $p_T > 10$ GeV. The $\Upsilon(1S)$ polarization parameter is relatively more negative in both cases, but the statistical uncertainties preclude any definite statements about depolarization of the ground state. There is a suggestion of an offset between the $p\bar{p}$ and pp polarization parameters in the Υ case, most clearly in the $\Upsilon(1S)$ case. This may indicate a dependence on having a p or \bar{p} target.

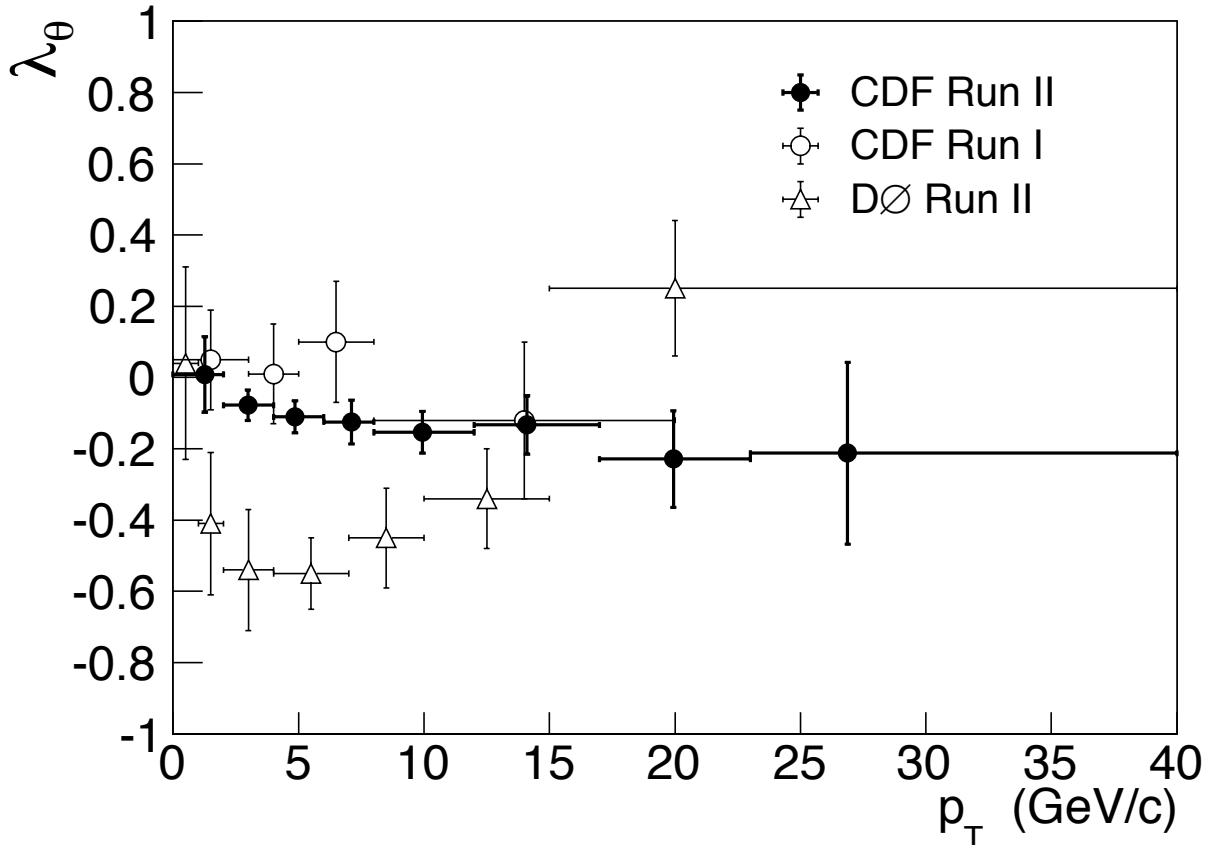


FIG. 3: Measurements of λ_θ in the cm-helicity frame for the $\Upsilon(1S)$ for the three Tevatron experiments: CDF Run 1, CDF Run 2, and D0 Run 2.

In Fig. 5, we plot the λ_θ parameters for the CMS and CDF measurements in the cm-helicity frame for the $1S$ states of bottomonium and charmonium as a function of the transverse mass $m_T = \sqrt{m^2 + p_T^2}$. We also plot λ_θ measurements for J/ψ and $\Upsilon(1S)$ in the CS frame as a function of m_T from CMS. The CDF J/ψ data are not available in the CS frame. One sees two features in this figure: (a) in each experiment, the polarization parameters of the two onia ground states are nearly the same and show the same trend with m_T ; and (b) the trends in the cm-helicity frame are different for pp and $p\bar{p}$. The pp results are consistent with no m_T dependence and a constant $\lambda_\theta = 0.13 \pm 0.04$. The $p\bar{p}$ λ_θ parameter shows a linear decrease starting at zero near $m_T = 7$ GeV with a slope of $(-0.015 \pm 0.003)/\text{GeV}$. Again, this *may* indicate a target-dependent effect that makes the polarization different for pp and $p\bar{p}$. For both types of target, the polarization mechanism at large m_T seems to be independent of heavy-quark flavor, since the J/ψ and $\Upsilon(1S)$ polarization parameters follow the same pattern for each target particle.

E. Discussion

We have seen some interesting systematic features of quarkonium polarization emerge from the comparison of the many available measurements at low p_T and from the large- p_T collider experiments. To reiterate, they include

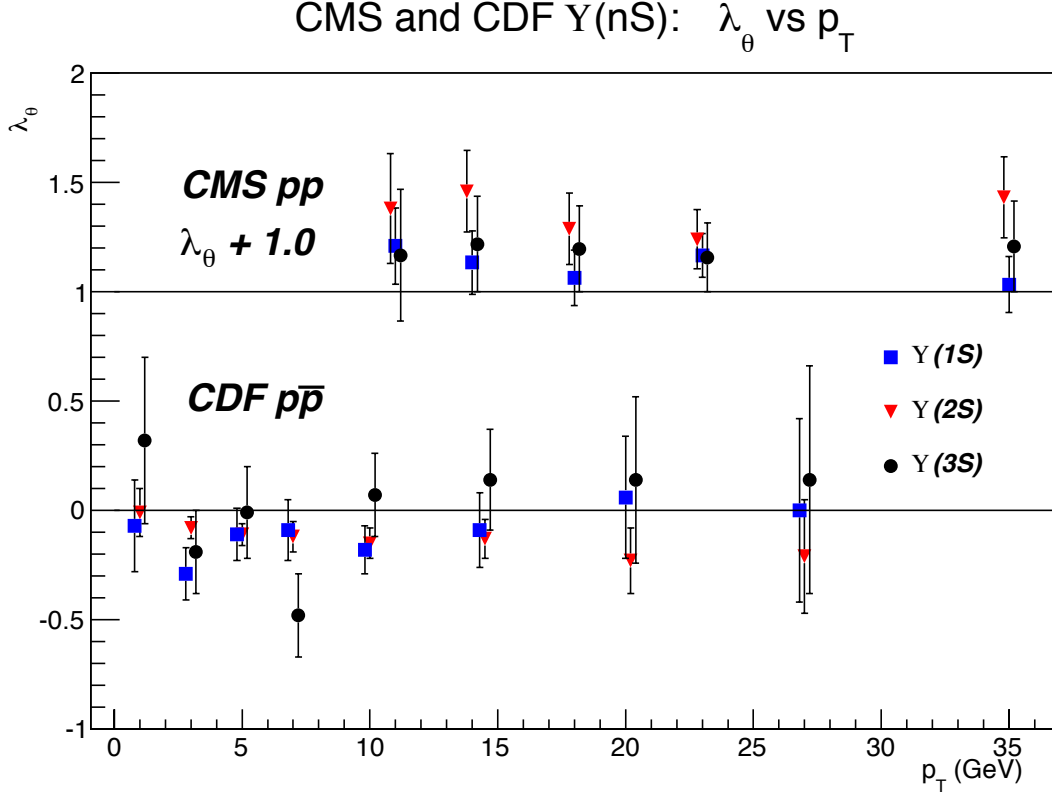


FIG. 4: Comparison of λ_θ parameters in the cm-helicity frame for $\Upsilon(nS)$ production from CDF Run 2 for $p\bar{p}$ production and from CMS for pp production. For clarity of presentation, the CMS values have had 1.0 added to each λ_θ measurement. Also, for both sets of data, the p_T values for $\Upsilon(2S)$ and $\Upsilon(3S)$ have been shifted left and right by 0.2 GeV, respectively.

- With the exception of the NuSea pCu bottomonium measurement, all of the measured polarization parameters in the cm-helicity or CS frames from any experiment are small for the p_T range of 1–70 GeV. Furthermore, there is little p_T -variation among the measurements from pp collisions within the uncertainties.
- For $p_T < 10$ GeV, it is striking that the J/ψ polarization parameter λ_θ in the cm-helicity frame shown in Fig. 2 is almost independent of target particle or rapidity range and tends to be p_T -independent for $1 < p_T < 10$ GeV. Those experiments that measured λ_θ in the CS frame found it to be also small, so the polarization in this p_T range is not large in any reference frame.
- As shown in Fig. 4 for the cm-helicity frame, the λ_θ measurements for the three $\Upsilon(nS)$ states show little variation with p_T or principal quantum number n in either pp or $p\bar{p}$ interactions.
- At comparable m_T values, the polarization parameters for ground-state charmonium (J/ψ) and ground-state bottomonium ($\Upsilon(1S)$) are consistent with each other and show little variation for $m_T > 10$ GeV. We had noted earlier that the measured feeddown fractions in $p\bar{p}$ experiments for the two quarkonium ground-state systems are equal within measurement uncertainties.

CMS and CDF: J/ψ and $\Upsilon(1S)$ λ_θ vs m_T

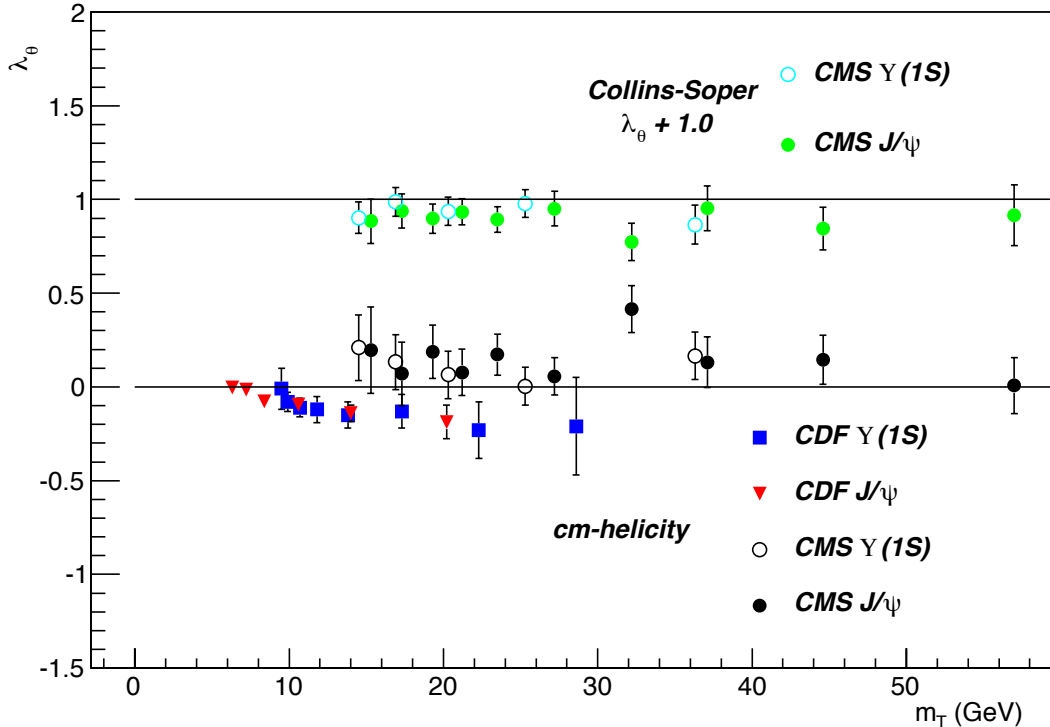


FIG. 5: Comparison of λ_θ parameters in the cm-helicity and Collins-Soper frames as functions of the transverse mass m_T for J/ψ and for $\Upsilon(1S)$. The data are from CDF Run 2 and from CMS. For clarity of presentation, the Collins-Soper values have had 1.0 added to each λ_θ measurement.

- For $\Upsilon(nS)$ production, there is a suggestion of a difference in polarization parameters between pp measurements from CMS and $p\bar{p}$ measurements from CDF.

VI. SUMMARY

A. Future Experimental Directions

The question of to what extent feeddown influences the polarization of the lowest-lying quarkonium states has been raised repeatedly. The best chance to measure these effects seems to be in the large datasets collected at the LHC. Colliding beam experiments at the Tevatron and LHC have identified radiative decays of P -wave quarkonium states to the S -wave ground state using photon conversions in the material of the inner tracker. With larger data sets yet unanalyzed, one might hope to measure the polarization of the ground-state quarkonia that result from P -wave decay sources. We see in Fig. 5 that the polarization parameters of the $\Upsilon(1S)$ and J/ψ mesons for $m_T > 10$ GeV are consistent with each other and have little variation with p_T in either the cm-helicity or CS frames. A first step in understanding feeddown effects would be to measure the polarization of the J/ψ produced from χ_c decays and of $\Upsilon(1S)$ produced from $\chi_b(1P)$ decays, using conversion photons combined with reconstructed dimuon events to identify the P -wave parent event

candidates. One need not separate the χ_{QJ} states with different J . There are already measurements of the $J = 2$ to $J = 1$ ratios for the χ_c at the Tevatron and LHC. We encourage the experimenters to pursue the determination of the J/ψ polarization in χ_c events and to extend the studies to measure the $\Upsilon(1S)$ polarization in χ_b radiative decays. From the results that we have seen, it should be adequate to measure λ_θ with respect to two spin-quantization axes, the CS frame and either the cm-helicity frame or, if the measurements extend out to large rapidity, the \perp -helicity frame. Because one is not measuring a cross section but rather a ratio of longitudinal and transverse polarization contributions, the absolute photon conversion efficiency is not needed. A good determination of the energy dependence of the conversion efficiency is crucial, though, to handle the range of photon energies for candidate events. The fundamental question is whether the polarization from these decays is different from the inclusive prompt polarization for the J/ψ or $\Upsilon(1S)$. The answer will directly aid future theoretical analysis of quarkonium polarization.

The experimental comparisons of the present data suggest some additional studies using existing data. They include:

- A new CDF measurement of J/ψ and $\psi(2S)$ polarization could gain an order of magnitude more statistics if it were redone using the full Tevatron data set. The increased statistics would allow the determination of all three polarization parameters in the analysis, and results could be reported in several frames. It should also be possible to measure the $\psi(2S)$ polarization parameters with the larger data set. It is not clear if D0 has sufficient mass resolution to do such a study, but it would be a useful check if it were possible.
- LHCb can lower the measurement uncertainty on its smallest rapidity bin using the complete LHC dataset. This would help to evaluate a possible change of polarization with rapidity that cannot be excluded by the present measurements.
- CMS can increase the statistics for its J/ψ polarization measurement to decrease the lower p_T cutoff of its measurement, especially for a range of rapidity closer to the LHCb lower limit of $y = 2$, to investigate the polarization behavior in this potential transition region. Also, reducing the uncertainty on the measurements would address the question of whether there is a target dependence in the polarization parameters between pp and $p\bar{p}$ measurements.

The Tevatron and LHC experiments have developed impressive analysis techniques and have detectors that work extremely well for the subtle business of analyzing polarization. Applying these tools to available data could go far in helping to understand the details of polarization in the production of quarkonium in hadronic collisions.

B. Theory Outlook

The predictions for quarkonium polarization from NRQCD factorization at NLO are not in dramatic disagreement with the data, but the differences are in many cases significant, given the current experimental and theoretical error bars. As the experimental uncertainties decrease with higher statistics, accommodating the data will be increasingly challenging for theory. As the range of the measurements is extended to higher p_T , there is still an opportunity for theory to predict the polarization.

The NRQCD factorization approach to quarkonium production has been pushed to NLO in α_s , thanks to heroic NLO calculations of the pQCD cross sections by three groups independently. The predictions for polarization at NLO differ dramatically from those at LO. This raises the question of whether N²LO corrections could be important. Unfortunately, the calculation of the pQCD cross sections at N²LO may be prohibitively difficult.

The NLP fragmentation formula, in conjunction with the NRQCD expansion of the fragmentation functions, provides a new framework for quarkonium production at large p_T . Predictions for quarkonium production, with pQCD cross sections calculated to NLO in $\alpha_s(p_T)$ and fragmentation functions calculated to NLO in $\alpha_s(m_Q)$, should be available soon. It will be interesting to see how the predictions for polarization compare to those from NRQCD factorization at NLO. Since this approach separates the scales p_T and m_Q , reducing calculations of the pQCD cross sections and the fragmentation functions to single-scale problems, calculations to N²LO in α_s may be tractable.

Quantitative predictions of the polarization depend on the choice of data used to determine the NRQCD matrix elements. The safest choices from a theoretical perspective are data involving the largest p_T 's. If the data are restricted to spin-summed cross sections at the large p_T 's that are accessible only at the Tevatron and the LHC, the error bars on polarization predictions are very large. If polarization measurements are included in the fitting data, there is still some predictive power in the dependence of the polarization on p_T . Testing these predictions requires measurements out to the largest values of p_T possible.

Current polarization measurements are for the inclusive production of quarkonium. The sum over all additional hadrons, together with the integration over parton momentum fractions, tends to wash out the polarization signal. The polarization signal could be enhanced by taking into account more information about the final-state hadrons, such as the direction of the hardest jet that balances most of the transverse momentum [9]. In associated production of quarkonium with another particle, such as a Z^0 [69], one could also exploit the momentum vector of the associated particle.

C. Concluding Remarks

The polarization studies from the wide range of experiments covered in this review produce a surprisingly coherent picture of quarkonium polarization over a wide range of p_T . No experiment observes large polarization in any reference frame for either quarkonium flavor (except NuSea in pCu collisions). Nevertheless, the polarization parameters in the high-precision experiments (CDF Run 2, CMS) are not zero. The theoretical treatment of polarization is on its firmest footing at very large p_T . There are opportunities at the LHC to extend the present measurements into an even higher p_T range, as well as to improve the measurement precision by having larger datasets. In conjunction with theoretical improvements, they may allow us to finally develop a clear picture of how quarkonium states are produced in hadronic collisions.

Acknowledgements

James Russ would like to acknowledge the contributions of his colleagues in the CMS and CDF collaborations in many fruitful discussions. His work was supported in part by the U.S. Department of Energy under Grant No. de-sc0010118TDD. Eric Braaten would like to

acknowledge discussions with Geoff Bodwin. Braaten's work was supported in part by the U.S. Department of Energy under grant DE-FG02-05ER15715.

- [1] Kosowsky A. *New Astron. Rev.* 43:157 (1999)
- [2] Faccioli P, Lourenco C, Seixas J, Wohri HK. *Eur. Phys. J. C* 69:657 (2010)
- [3] Palestini S. *Phys. Rev. D* 83:031503 (2011)
- [4] Faccioli P, Lourenco C, Seixas J. *Phys. Rev. D* 81:111502 (2010)
- [5] Faccioli P, Lourenco C, Seixas J. *Phys. Rev. Lett.* 105:061601 (2010)
- [6] Gottfried K, Jackson JD. *Nuovo Cim.* 33:309 (1964)
- [7] Collins JC, Soper DE. *Phys. Rev. D* 16:2219 (1977)
- [8] Braaten E, Kang D, Lee J, Yu C. *Phys. Rev. D* 79:014025 (2009)
- [9] Braaten E, Kang D, Lee J, Yu C. *Phys. Rev. D* 79:054013 (2009)
- [10] Faccioli P, Lourenco C, Seixas J, Wohri, HK. *Phys. Rev. Lett.* 102:151802 (2009)
- [11] Lepage GL, et al. *Phys. Rev. D* 46:4052 (1992)
- [12] Bodwin GT, Braaten E, Lepage GP. *Phys. Rev. D* 51:1125 (1995) [*Erratum-ibid. D* 55:5853 (1997)]
- [13] Bodwin, GT et al. arXiv:1307.7425
- [14] Nayak GC, Qiu J-W, Sterman GF. *Phys. Lett. B* 613:45 (2005)
- [15] Nayak GC, Qiu J-W, Sterman GF. *Phys. Rev. D* 72:114012 (2005)
- [16] Braaten E, Yuan TC. *Phys. Rev. Lett.* 71:1673 (1993)
- [17] Braaten E, Cheung K-M, Yuan TC. *Phys. Rev. D* 48:4230 (1993)
- [18] Braaten E, Lee J. *Nucl. Phys. B* 586:427 (2000)
- [19] Braaten E, Fleming S. *Phys. Rev. Lett.* 74:3327 (1995)
- [20] Cho PL, Wise MB. *Phys. Lett. B* 346:129 (1995)
- [21] Kang Z-B, Qiu J-W, Sterman G. *Nucl. Phys. Proc. Suppl.* 214:39 (2011)
- [22] Kang Z-B, Qiu J-W, Sterman GF. *Phys. Rev. Lett.* 108:102002 (2012)
- [23] Fleming S, Leibovich AK, Mehen T, Rothstein IZ. *Phys. Rev. D* 86:094012 (2012)
- [24] Fleming S, Leibovich AK, Mehen T, Rothstein IZ. *Phys. Rev. D* 87:074022 (2013)
- [25] Ma Y-Q, Qiu J-W, Zhang H. arXiv:1311.7078 [hep-ph]
- [26] Ma Y-Q, Qiu J-W, Zhang H. arXiv:1401.0524 [hep-ph]
- [27] Kang Z-B, Qiu J-W, Ma Y-Q, Sterman G. arXiv:1401.0923 [hep-ph]
- [28] Kartvelishvili VG, Likhoded AK, Slabospitsky SR. *Sov. J. Nucl. Phys.* 28:678 (1978) [*Yad. Fiz.* 28:1315 (1978)]
- [29] Chang C-H. *Nucl. Phys. B* 172:425 (1980)
- [30] Berger EL, Jones DL. *Phys. Rev. D* 23:1521 (1981)
- [31] Baier R, Ruckl R. *Phys. Lett. B* 102:364 (1981).
- [32] Artoisenet P et al. *Phys. Rev. Lett.* 101:152001 (2008)
- [33] Lansberg JP. *Phys. Lett. B* 695:149 (2011)
- [34] Butenschoen M, Kniehl BF. *Phys. Rev. Lett.* 108:172002 (2012)
- [35] Gong B, Wang J-X. *Phys. Rev. Lett.* 100:232001 (2008)
- [36] Fritzsche H. *Phys. Lett. B* 67:217 (1977)
- [37] Halzen F. *Phys. Lett. B* 69:105, (1977)
- [38] Bodwin GT, Braaten E, Lee J. *Phys. Rev. D* 72:014004 (2005)
- [39] Baranov SP, Zotov NP. *JETP Lett.* 86:435 (2007)

- [40] Baranov SP, Zotov NP. *JETP Lett.* 88:711 (2008)
- [41] Braaten E, Kniehl BA, Lee J. *Phys. Rev. D* 62:094005 (2000)
- [42] Kniehl BA, Lee J. *Phys. Rev. D* 62:114027 (2000)
- [43] Braaten E, Lee J. *Phys. Rev. D* 63:071501 (2001)
- [44] Butenschoen M, Kniehl BA. *Phys. Rev. Lett.* 106:022003 (2011)
- [45] Ma Y-Q, Wang K, Chao K-T. *Phys. Rev. D* 84:114001 (2011)
- [46] Gong B, Wan L-P, Wang J-X, Zhang H-F. *Phys. Rev. Lett.* 110:042002 (2013)
- [47] Chao K-T, et al. *Phys. Rev. Lett.* 108:242004 (2012)
- [48] Gong B, Wan L-P, Wang J-X, Zhang H-F. arXiv:1305.0748 [hep-ph]
- [49] Agostellini, S et al. *Nucl. Instrum. Meth. A* 506:250 (2003)
- [50] Lange, DJ. *Nucl. Instrum. Meth. A* 462:152 (2001)
- [51] Sjostrand T, Mrenna S, Skands PZ. *JHEP* 0605:026 (2006)
- [52] Affolder T et al. CDF Collaboration. *Phys. Rev. Lett.* 85:2886 (2000)
- [53] Chang TH et al. NuSea Collaboration. *Phys. Rev. Lett.* 91:211801 (2003)
- [54] Brown, CN et al. NuSea Collaboration. *Phys. Rev. Lett.* 86:2529 (2001)
- [55] Abt I. et al. HERA-B Collaboration. *Eur. Phys. J. C* 60:517 (2009)
- [56] McGaughey PL, Moss JM, Peng JC. *Annu. Rev. Nucl. Part Sci.* 21:400 (2008)
- [57] Abe F et al. CDF Collaboration. *Phys. Rev. Lett.* 79:572 (1997)
- [58] Abachi S et al. D0 Collaboration. *Phys. Lett. B* 380:239 (1996)
- [59] Affolder T et al. CDF Collaboration. *Phys. Rev. Lett.* 84:2094 (2000)
- [60] Acosta D et al. CDF Collaboration. *Phys. Rev. Lett.* 88:161802 (2002)
- [61] Abazov VM et al. D0 Collaboration. *Phys. Rev. Lett.* 101:182004 (2008)
- [62] Abulencia A et al. CDF Collaboration. *Phys. Rev. Lett.* 99:132001 (2007)
- [63] Aaltonen T et al. CDF Collaboration. *Phys. Rev. Lett.* 108:151802 (2012)
- [64] Chatrchyan S et al. CMS Collaboration. *Phys. Rev. Lett.* 110:081802 (2013)
- [65] Chatrchyan S et al. CMS Collaboration. *Phys. Lett. B* 727:381 (2013)
- [66] Abelev B et al. ALICE Collaboration. *Phys. Rev. Lett.* 108:082001 (2012)
- [67] Aaij R et al. LHCb Collaboration. *Eur. Phys. J. C* 73:2631 (2013)
- [68] Adare A et al. PHENIX Collaboration. *Phys. Rev. D* 82:012001 (2010)
- [69] Gong B, Lansberg JP, Lorce C, Wang J. *JHEP* 1303:115 (2013)